1

Ion Selectivity and Conductance

Alexander A. Simon, Chen Fan, Dorothy M. Kim, Jason G. McCoy, and Crina M. Nimigean

CONTENTS

1.1 Introduction

Ion channels function to orchestrate an exquisite array of physiological processes, including nerve impulses, muscle contraction, regulation of cell volume, and cell signaling in all organisms. The electric current in a signaling event is generated by fast ion fluxes across the cell membrane controlled by the opening and closing of ion channels, including those permeable to potassium (K^+), sodium (Na^+), calcium (Ca^{2+}), and chloride (Cl^-) ions. The direction of the ion fluxes is determined by preset transmembrane ionic gradients established by passive transport through specific K^+ channels plus the Na^+/K^+ ATPase that pumps ions against their concentration gradients through hydrolysis of adenosine triphosphate (Figure 1.1). For certain signaling modes—such as the generation of the action potential—it is important that the ion channels involved are mostly permeable to a specific ion and have a high ion conducting rate.

As early as 1902, Julius Bernstein predicted that a change in membrane permeability resulted in an electrical excitation of the membrane. Bernstein hypothesized that cells at rest were only permeable to K^+ ions and permeability to other ions occurred during excitation. This provided the first suggestion of ion-selective components in the membrane (Bernstein 1902) (Figure 1.1). Breakthrough studies on the squid giant axon in the 1940s and 1950s identified the action potential in the axon to be the result of a composite of currents carried by different ions. Using the voltage-clamp technique, Alan Hodgkin and Andrew Huxley developed a model directly correlating Na^+ and K^+ fluxes with excitation

DOI: 10.1201/9781003096214-2

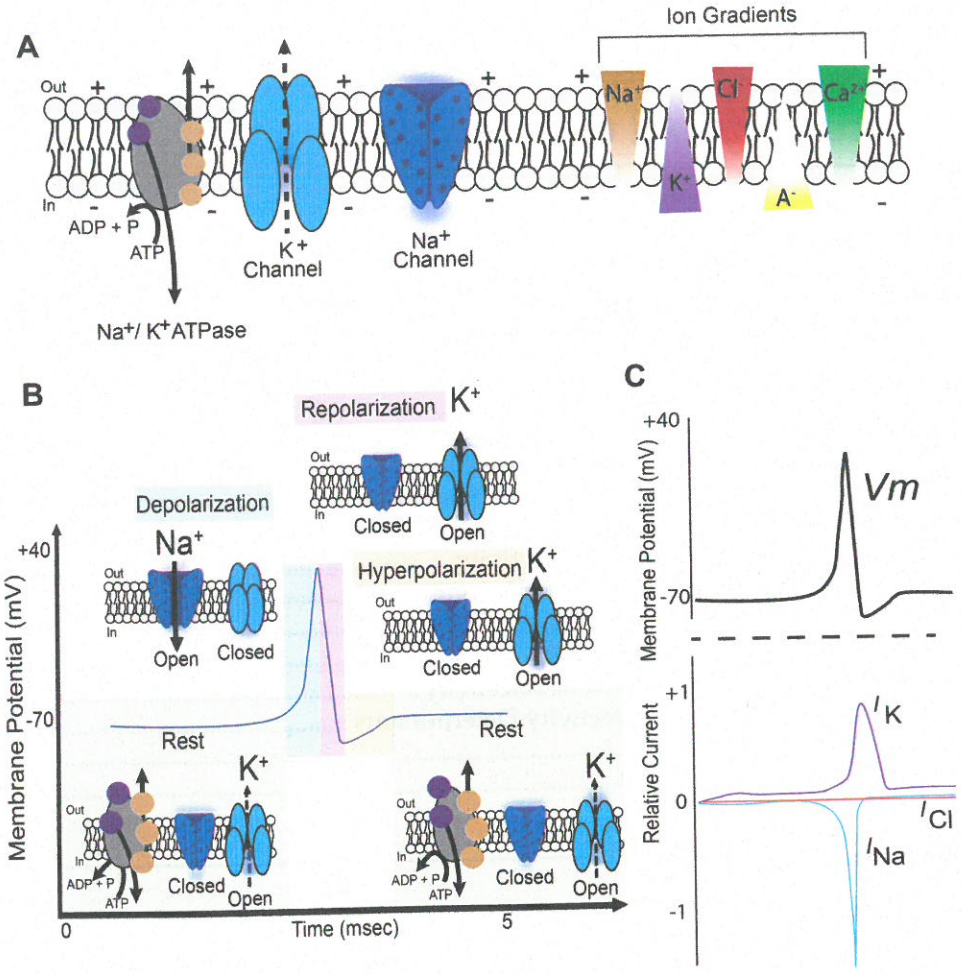

FIGURE 1.1
Ion flux choreography in a typical neuron at rest and during an action potential. (A) Na^+/K^+ ATPase and K^+ channels regulate the resting state of the membrane to establish standing ion gradients—particularly of Na^+ and K^+—across the membrane and maintain a charge separation resulting in a negatively charged interior. The Na^+/K^+ ATPase transports Na^+ (brown spheres) out of the cell and K^+ (purple spheres) into the cell with a 3:2 stoichiometry, respectively. The presence of large organic anions (A^-) in the intracellular space likewise contribute to a negative resting potential. Although gradients of other ions (Ca^{2+}, Cl^-) exist and are pivotal to other physiological processes in electrochemical signaling cascades, their low permeabilities across the membrane at rest minimize their contribution to the steady-state transmembrane potential according to the Goldman–Hodgkin–Katz equation. (B) General schematic of ion channel opening and closing during an action potential. In both (A) and (B), dashed lines through K^+ channels indicate a "leak" or background current. (C) Representation of the membrane potential changes (top) mirrored against corresponding ionic currents (bottom). Upward deflections represent outward currents, while downward deflections are inward currents by convention.

and electric conduction along the axon, earning them the Nobel Prize in 1963. They concluded that the resting membrane was indeed predominantly selective to K^+ ions, resulting in a negative transmembrane potential (according to the electrophysiological convention, the transmembrane potential is measured inside the cell relative to the outside). On the other hand, Na^+ ions were responsible for the inward current causing the cell membrane to become more positive than at rest, referred to as depolarization (Hodgkin and Huxley

1952; Hodgkin and Keynes 1955) (Figure 1.1B). These studies revealed a choreography of ion fluxes across the cell membrane underpins the electrical propagation and the fluxes would need to be associated with highly selective ion channels to maintain the observed specificity.

Shortly thereafter, in the 1970s, ion channels selective for Na^+ and Ca^{2+} were purified from membrane preparations. It was not until the 1980s that the first ion channel genes encoding a nicotinic acetylcholine receptor (nAChR) from *Torpedo californica* and a voltage-gated Na^+ (Na_v) channel from the electric eel *Electrophorus electricus* were cloned (Noda et al. 1984; Noda et al. 1982). The cation channel forming nAChR was also the first to be recorded with patch clamping at the single-channel level from native membranes, and then eventually purified, reconstituted, and recorded in a lipid bilayer (Montal et al. 1984; Neher and Sakmann 1976).

The first protein specifically involved in the conductance of K^+ was discovered through genetic analysis of *Drosophila* mutants exhibiting a neuromuscular defect manifested through uncontrollable shaking. The region of genomic DNA carrying the gene of interest became known as the *Shaker* locus and it encoded a member of the voltage-gated potassium channel (K_v) family. The encoded Shaker protein was also the first K^+ channel to be cloned (Papazian et al. 1987). Molecular cloning of these ion channels allowed for functional characterizations and was the foundation for deciphering structure–function mechanisms. Notably, heterologous expression of a K^+ channel for patch-clamp recordings revealed a clear selection preference for K^+, Rb^+, and NH_4^+ over Na^+ not observed in the other cation channel types (Heginbotham et al. 1994). The genetic and electrophysiological evidence provided by these studies on Na^+, Ca^{2+}, and K^+ channels enabled powerful taxonomic grouping of known channels into functional superfamilies as well as the predictions of novel channels by sequence analysis that became targets for subsequent cloning, providing a rich trove of amino acid sequence information. The rapid accumulation of information in the era of cloning led to a major achievement in the first crystal structure of an ion channel in 1998 (Doyle et al. 1998).

1.2 Structural Basis for Selectivity in K^+ Channels

The key for understanding the mechanism of selectivity in channels lies in the aqueous pore, a narrow canal comprising the permeation path for ions across a hydrophobic membrane (Figure 1.2A,B). The simplest illustration of the pore is that of a molecular sieve that can only pass ions not exceeding a certain radius (Figure 1.2C). Although pore size was initially found to be a major determinant of ion permeability, it was insufficient to explain the permeability sequences determined for some channels. The region within the channel pore that directly interacts with the conducting ions is called the selectivity filter, and both the dimensions and chemical properties of this region influence ion selectivity.

Prior to the elucidation of the atomic structures of ion channels, one early hypothesis asserted that for channels to discriminate between ions they would need to dehydrate upon entry into the pore (Bezanilla and Armstrong 1972). The energy required for this step would need to be compensated for by stabilizing interactions between the ion and the walls of the pore (Eisenman 1962). Binding sites contained in the pore and selectivity filter would only accommodate ions of certain size and valence, and consequently require ions to overcome various energy barriers to permeate the pore. Thus, the pore provides an

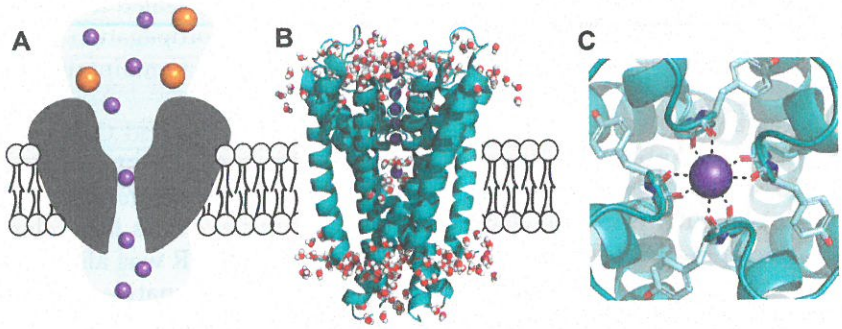

FIGURE 1.2
A model K^+ channel. (A) Cartoon of a simplified ion channel envisioned as the molecular sieve based on early functional electrophysiology studies. Small purple spheres represent permeant ions and large orange spheres represent non-permeant ions. (B) Side view of the K^+ selective ion channel, KcsA, determined by X-ray crystallography constituting an aqueous passageway spanning a lipid membrane. K^+ ions (purple spheres) within the selectivity filter form a single-file line. Water molecules are depicted with an oxygen atom shown as a red sphere and two hydrogen atoms as gray spheres. (C) Close-up view of K^+ ion within the selectivity filter at position S1 viewed from the extracellular side of the membrane.

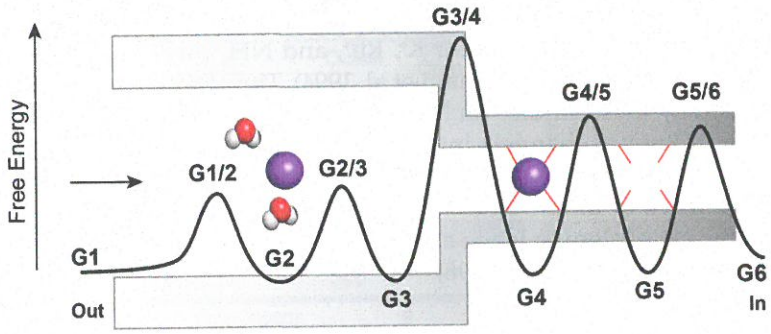

FIGURE 1.3
Energy landscape. Hypothetical energy landscape of an ion (purple sphere) traversing an envisioned form of a simplified ion channel pore with narrow selectivity filter. Ion-binding sites are shown as red sticks. A large energy barrier is indicated for ion dehydration and entry into selectivity filter.

energy landscape that favors permeation of certain ions. Within the energy landscape, ion-binding sites represent energetic minima separated by energetic barriers that can also be encountered upon entering and exiting the pore (Hille 2001) (Figure 1.3). Ions with lower permeability may face a higher energy barrier at external binding sites or alternatively may encounter very deep energy wells within the selectivity filter (Figure 1.3). The differential energy barriers experienced by various ions can also explain why channels often are permeable to several ions but have a preferential selectivity sequence.

The predicted binding sites "stabilizing" dehydrated K^+ ions would be composed of a "bracelet" of oxygen dipoles within the selectivity filter region of the K^+ channel pore (Bezanilla and Armstrong 1972). The selectivity filter would also be of a cylindrical shape with an inner diameter between 3.0 and 3.4 Å (shown in Figure 1.4A, in direct comparison with the predicted structure of a Na^+ channel selectivity filter in Figure 1.4D). Later, the selectivity filter was identified on the "P-loop" containing a highly conserved signature sequence of amino acids—TVGYG—that could contribute oxygen dipoles and found to instigate distinct changes in ion selectivity upon mutation (Heginbotham et al. 1994).

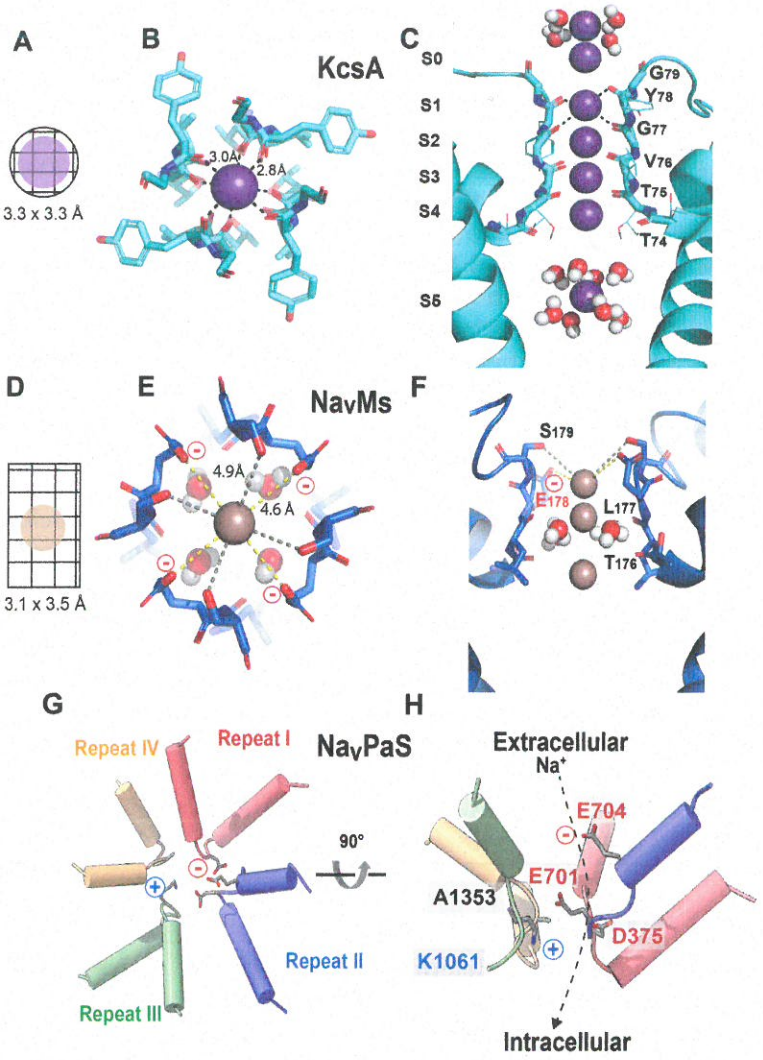

FIGURE 1.4

Pore dimensions and ion selectivity. (A and D) Predicted pore dimensions of a K^+ and Na^+ channel, respectively, based on Dwyer et al. (1980). (B and E) Structural determinations of a prokaryotic K^+ channel pore (KcsA, PDB: 1K4C) and prokaryotic Na^+ channel pore (Na_vMs, PDB: 5HVX) viewed for the extracellular side of the membrane. Both tetrameric structures are symmetric. (C) Close-up view of the KcsA selectivity filter comprised of TTVGYG sequence. Symmetrical subunits form a narrow constriction requiring the dehydration of ions and holds four K^+ ion-binding sites (S1, S2, S3, S4) coordinated by the carbonyl backbones of the signature sequence. (F) Close-up view of the Na_vMs selectivity filter designated by residues TLES from a side view showing a partially hydrated selectivity filter where multiple bound ions are largely coordinated by amino acid side chains, particularly the high field strength anion of glutamate. Yellow dashed line in (E, F) represents bond between ion and the negatively charged glutamate that comprises the characteristic EEEE ring of prokaryotic Na^+ channels. In both (C) and (F), only two opposing subunits are displayed for clarity. (G and H) Top and side views of the asymmetric selectivity filter of the eukaryotic Na_vPaS channel (PDB: 6A90). The four repeats are colored differently, critical residues are shown as sticks and labeled. The negative and positive charges are indicated. The proposed Na^+ conduction pathway is indicated by a dashed line.

These predictions—based entirely on functional data—turned out to be astonishingly accurate and were supported by the crystal structure of the KcsA potassium channel (Figure 1.4B, C).

The KcsA crystal structure revealed a selectivity filter with a radius of ~3 Å, formed by four symmetrical P-loops to harbor K^+ binding sites, which may not accommodate Na^+ ions or other large cations like Cs^+ or Ba^{2+} (Doyle et al. 1998; Zhou et al. 2001). The specific K^+ binding sites were formed by the backbone carbonyls of residues from the signature sequence that point directly into the center of the protein at its narrowest point (Doyle et al. 1998; Morais-Cabral, Zhou, and MacKinnon 2001). Oxygen dipoles coordinated the dehydrated K^+ ions in a cage-like structure by surrounding each K^+ ion with eight oxygen atoms (two from each subunit) (Doyle et al. 1998; Zhou et al. 2001). In addition to the four K^+ ions fully coordinated by the protein (at sites S1–S4), a fifth K^+ binding site (S0) at the extracellular surface of the channel was coordinated by the backbone carbonyl oxygens of a tyrosine and four water molecules (Figure 1.4B, C).

Structural data, in conjunction with the wealth of structure-based data that followed, revolutionized the ion channel field and inspired many new avenues of research. The structure of the KcsA potassium channel and the three-dimensional architecture of the selectivity filter yielded a detailed picture of the molecular mechanisms by which K^+ channels distinguish between different ions. These structures confirmed many of the predictions of early functional data including the physical properties of the pore such as the identities of functional groups that interact with the K^+ ions and the bond distances, the dehydration of ions within the selectivity filter, and the multi-ion nature of ion conduction. Moreover, they also serve as good starting models for molecular dynamic simulations, which can also provide a detailed understanding of selectivity.

1.3 Structural Basis for Selectivity in Na^+ Channels

Electrophysiological experiments determining permeability ratios indicated that Na_v channels can accommodate many different cations and have a large pore. These studies hypothesized that the Na^+ channel contains a rectangular opening of approximately 3 × 5 Å surrounded by oxygen atoms as well as a negatively charged carboxylate ion (Dwyer, Adams, and Hille 1980) (Figure 1.4D, E). The size of this opening further suggested that the Na^+ ions conduct in a partially hydrated state. K^+ channels, on the other hand, were observed to contain a narrower pore than Na^+ channels resulting in higher selectivity due to increased interaction and contact between the ion and the pore walls (Hille 2001) (Figure 1.4A–C). This prediction of relative pore size between Na^+ and K^+ channels was later confirmed by the crystal structures of Na_v channels from bacteria, which have a selectivity filter that is ~4.6 Å wide (Payandeh et al. 2011) (Figure 1.4E). More recent structures captured by cryo-electron microscopy (cryo-EM) confirm a water density around a Na^+ ion suggesting ions enter the pore in a partially hydrated state, collectively supporting hypotheses for mechanisms of ion selectivity based on pore diameter and ion hydration (Sula et al. 2017) (Figure 1.4E, F). Furthermore, since the selectivity sequence of Na^+ channels (Na^+~Li^+ > Tl^+ > K^+ >> Ca^{2+}) closely follows the electrostatic model of Eisenman, it was argued that selectivity was also dependent on the field strength of the binding site (Eisenman 1962). A high-field-strength anion, such as a glutamate side chain, would be required to increase the Na^+ selectivity relative to that of K^+.

Characteristic of several bacterial Na_v channels is a tetrameric architecture and a glutamate residue in the signature position within the selectivity filter, similar to eukaryotic Ca^{2+} channels. A ring of four glutamates (EEEE)—one glutamate from each of the four subunits—is positioned along the pore in the center of the channel near the extracellular opening (Figure 1.4E, F). The cavity between the four glutamate side chains is the most constricted region within the channel allowing just enough room for the conducting Na^+ to remain partially hydrated while directly interacting with one of the glutamates. Mutagenesis experiments illustrated the glutamate residue was responsible for Na^+ permeation relative to Ca^{2+} (Naylor et al. 2016). Interior to this glutamate, the backbone carbonyl oxygens of the two following amino acids (Leu and Thr) point into the pore (Figure 1.4F). Solvent molecules coordinated to these carbonyl oxygens presumably help rehydrate the Na^+ ion as it passes through the filter. The similarity of the EEEE sequence of prokaryotic Na_v channels that shows more homology to eukaryotic voltage-gated Ca^{2+} channels than eukaryotic Na_v channels invites questions regarding the evolutionary origins of Na^+ and Ca^{2+} channels. The similarities in the selectively filter further suggest that there are additional features that tune selectivity for Na^+ versus Ca^{2+}.

Cloning and sequencing of mammalian Na_v channels led to the identification of four key residues instrumental in maintaining Na^+ selectivity. These residues consist of an aspartate, a glutamate, a lysine, and an alanine that form the DEKA motif. Unlike K^+ channels and the bacterial Na^+ channels, eukaryotic Na^+ channels are monomeric proteins containing four similar repeated domains, thus lacking the fourfold symmetry (Figure 1.4G). Each residue of the DEKA motif is in a distinct domain starting with the aspartate in the N-terminal-most repeat but occupies the same location in the primary structure based on sequence alignments of each individual domain. As Hille predicted, the filter sequence contains two residues with carboxyl-containing side chains that evidently are conserved evolutionarily (Hille 2001). Mutations of the DEKA motif demonstrates its profound impacts on selectivity. Mutation of glutamate to alanine leads to an increase in K^+ permeability, while mutation of the aspartate to alanine has little effect. Glutamate therefore appears to play a larger role in selectivity in the Na^+ channel filter. Removal of the lysine side chain leads to an even greater loss in selectivity against K^+ as well as Ca^{2+} (Favre, Moczydlowski, and Schild 1996).

Recently, several Na_v channel structures from eukaryotes have been solved by cryo-EM (Shen et al. 2018; Pan et al. 2018). All these structures share similar asymmetric selectivity filter architectures lined by the side chains of the D,E,K,A signature residues found in repeats I to IV, respectively. In the Na_vPaS structure, the lysine (K_{1061}) side chain adopts a downward conformation, while an additional outer negatively charged glutamate residue (E_{704}) lies above the DEKA residues (Figure 1.4H). E_{704} guards the entrance to the selectivity filter vestibule by attracting cations and repelling anions allowing Na^+ coordination through a "DEE binding site" comprised of residues D_{375}, E_{701} and E_{704} (Shen et al. 2018) (Figure 1.4H). The DEE site is also predicted to comprise the energetic minimum along the ion conduction pathway (Zhang et al. 2018) (Figure 1.4H).

1.4 Mechanistic Models for Selectivity in Cation Channels

The aforedescribed structural data provides insights into selectivity mechanisms. There is now compelling evidence that key characteristics of the selectivity filter are observed in

both prokaryotic and eukaryotic K^+ channels. However, it remains to be seen to what extent all cation channels share evolutionary origins of selectivity as both quaternary structures and molecular properties diverged. Future studies pinpointing molecular mechanisms of ancestral prokaryotic channels in tandem with those focusing on the eukaryotic descendants are critical for identifying deviations. These discoveries are paramount for understanding the evolution of selectivity in ion channels. Next, we describe several models that have been proposed as the basis of selectivity. Many of these models are not necessarily mutually exclusive.

1.4.1 The Close-Fit Model for Selectivity

The underlying assumption of the close-fit model is that the selectivity filter distinguishes between different ions based on ionic radius. In this model, the distances between the conducting ion and the selectivity filter backbone carbonyl oxygens are tuned specifically to optimize the coordination for K^+ ions relative to that of smaller or larger ions (Figure 1.5). This partially alleviates the energetic penalty of dehydrating the K^+ ion required for entry into the selectivity filter. Despite this high affinity, the ions are still rapidly processed through the selectivity filter presumably due to electrostatic repulsions between multiple K^+ ions in close proximity in the filter. In the published 2 Å-resolution KcsA crystal

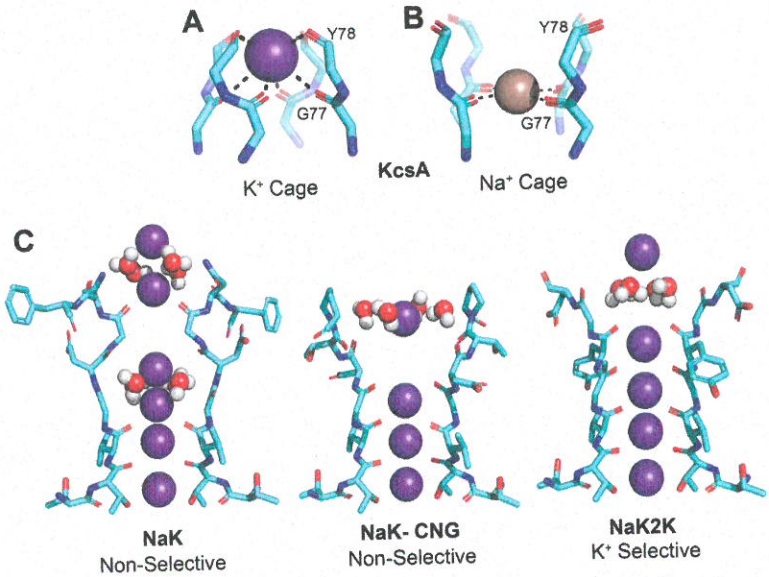

FIGURE 1.5
Selectivity models. (A) Ion coordination in the K^+ channel selectivity filter demonstrates close-fit, field-strength, coordination, and kinetic models. K^+ (purple sphere) binds with octahedral coordination in the center of a cage formed by eight carbonyl oxygens (left). In KcsA, the bond distance from G77 to the K^+ is 3.0 Å (PDB: 1K4C). (B) In contrast, Na^+ (tan sphere) binds with square planar coordination in the plane of the carbonyls (right). In the KcsA E71A variant, the bond distance from G77 to Na^+ is 2.5 Å (PDB: 3OGC). (C) Number of contiguous ion binding sites demonstrates the site number model of selectivity. The nonselective NaK channel (PDB: 3E8H) lacks the S1 and S2 binding sites (left panel). Restoration of the S2 site through mutagenesis of the selectivity filter to TVGDTPP (called NaK-CNG, PDB: 3K03), a sequence very similar to that of nonselective cyclic nucleotide-gated (CNG) channels fails to increase the K^+ selectivity of the channel (center). Restoration of site S1 through mutagenesis of the NaK selectivity filter to TVGYGDF (called NaK2K, PDB: 3OUFA), a sequence very similar to that of KcsA, results in a K^+ selective channel (right).

structure, the average coordination distance between the K^+ ions and the selectivity filter oxygen atoms range from 2.7 Å to 3.08 Å, nearly identical to that observed in the potassium-selective ionophores nonactin and valinomycin (Zhou et al. 2001). Na^+, with an ionic radius approximately 0.4 Å smaller than that of K^+, would require a positional shift of the selectivity filter in order to bind optimally. It should also be noted that crystal structures depict a positional average over time. Therefore, even though the structures show K^+ density in each of the selectivity filter binding sites, it is possible that the K^+ ions occupy only alternate binding sites as they pass through the channel (for example S4 and S2 or S3 and S1) (Morais-Cabral, Zhou, and MacKinnon 2001).

1.4.2 The Field-Strength Model for Selectivity

The field-strength model foregoes the idea of rigid cages (Figure 1.5A), and instead treats the selectivity filter as a flexible, "liquid-like" environment. The dipole moments of the selectivity filter backbone carbonyls generate electrostatic forces that repel each other and attract the cation leading to selectivity for K^+ (Noskov, Berneche, and Roux 2004). In this model, it is the physical properties of the ligand groups (i.e., the selectivity filter backbone carbonyls) that lead to selection for K^+ over other ions. In simplified simulations, a ligand dipole between 2.5 to 4.5 debye (similar to a carbonyl) selects for K^+, whereas decreasing or increasing the ligand dipole leads to optimal selection for larger or smaller cations, respectively (Noskov, Berneche, and Roux 2004).

1.4.3 The Coordination Model for Selectivity

The coordination model differs from the close-fit and field-strength models in that the number of groups that interact with the ligand also contributes to selectivity. In other words, a protein framework with eight liganding moieties, whether they belong to waters or carbonyls, as in the KcsA K^+ channel, will inherently select for K^+ over Na^+ (Bostick and Brooks 2007) (Figure 1.5A, B). In another version of the coordination model, the electric properties of the local environment of the binding sites create strong selectivity by over coordinating K^+ with eight carbonyl ligands instead of the usual six ligands coordinating K^+ in water (Varma, Sabo, and Rempe 2008).

1.4.4 Kinetic Model for Selectivity

In the aforedescribed selectivity mechanisms, the origins of selectivity are ultimately derived from a difference in the free energy of binding for different ions within the selectivity filter. An alternative kinetic-based model suggests that an additional layer of K^+ selectivity over other ions may be the result of a high-energy barrier preventing other ions from progressing through the selectivity filter. Molecular dynamics simulations of KcsA have predicted that the S4 site is slightly selective for both Na^+ and Li^+ over K^+; however, the energy minima for the Na^+ and Li^+ lies in the plane formed by the carbonyl oxygens dividing the S3 and S4 sites (Figure 1.5B) and supposed maxima at the preceding S1 or S2 (Thompson et al. 2009). Crystal structures of KcsA in the presence of Na^+ have also shown spherical densities between the carbonyl oxygens instead of centered in the carbonyl "cage" like K^+ (Cheng et al. 2011) (Figure 1.5A, B). The presence of K^+ may then occlude the preferred binding sites of smaller ions such as Na^+, generating a large Coulombic repulsion that prevents Na^+ from entering the selectivity filter (Thompson et al. 2009; Kim and Allen 2011).

1.4.5 The Site Number Model of Selectivity

Determination of the NaK channel crystal structure from *Bacillus cereus* led to the hypothesis of the site number model (Shi et al. 2006). Unlike KcsA, the NaK channel does not prefer K^+ to Na^+. This difference in selectivity appears to be largely due to a change in the sequence of the selectivity filter. The selectivity filter sequence in NaK is TVGDGNF, in contrast to the KcsA sequence of TVGYGDL. The result of this change is that sites S1 and S2 are disrupted, creating a large cavity in place of the two cage-like binding sites (Figure 1.5C). Modifying the NaK selectivity filter sequence to TVGDTPP—similar to what is observed in nonselective cyclic nucleotide-gated channels—reestablishes the S2 site but the channel still fails to demonstrate K^+ selectivity (Figure 1.5C). Modifying the NaK selectivity filter to TVGYGDF, similar to that of KcsA, reestablishes both the S1 and S2 sites, and results in heightened K^+ selectivity (Derebe et al. 2011) (Figure 1.5C). This suggests that the presence of four contiguous binding sites is a critical component for enacting K^+ selectivity.

1.4.6 Other K^+ Channel Selectivity Determinants

While it is clear that the selectivity filter is crucial to mediating channel selectivity, many aspects of selectivity cannot be explained entirely by the filter alone. Despite sharing the selectivity filter sequence TTVGYG, voltage-gated channel $K_v2.1$ conducts strong Na^+ currents in the absence of K^+, while $K_v1.5$, KcsA and Shaker do not (Korn and Ikeda 1995; Heginbotham and MacKinnon 1993; LeMasurier, Heginbotham, and Miller 2001). C-type inactivation, a process by which the selectivity filter changes conformation to halt K^+ conductance in response to prolonged opening of the channel, has also been shown to influence selectivity. Shaker channels, like many other members of the K_v family, can conduct Na^+ during C-type inactivation (Starkus et al. 1997). In contrast, Na^+ conduction can be increased in KcsA via a mutation behind the filter that rendered the channel non-inactivating (Cheng et al. 2011). Similarly, inward-rectifying K^+ channel $K_{ir}3.2$ was made permeable to Na^+ through mutation of a residue in the transmembrane helix behind the selectivity filter. The addition of a negatively charged amino acid into the $K_{ir}3.2$ channel cavity below the filter was able to restore K^+ selectivity (Bichet et al. 2006). These results demonstrate that residues beyond those forming the selectivity filter can influence ion selectivity and highlight the role that interactions between neighboring or distant amino acids have on the overall protein function.

1.5 Conductance

Ion conductance is a measure of the ease with which ions flow across the membrane. Ion conductance (g) typically given in units of picosiemens (pS) can be calculated from measurements of electrical current (I) generated by the movement of ions through the membrane normalized to the voltage (V) applied to the membrane simply by using a derivative of Ohm's law, $g = I/V$. In electrical terms, conductance is the inverse of resistance ($g = 1/R$). The ionic flux rate through a single ion channel—termed unitary conductance—can be measured by directly performing single-channel current measurements with patch-clamp or lipid bilayer recordings, or indirectly calculated from macroscopic currents using noise-analysis methods for determining the number of channels in a membrane (Neher and

Sakmann 1976; Silberberg and Magleby 1993). Comparisons of ion conductance among different channels are a useful first metric for comparing the ionic flux within their pores and offer a handle for understanding ion permeation paths.

Since conductance is given by the ionic flux, it generally increases with increasing permeant ion concentration. However, a linear relationship between conductance and ion concentration is not obeyed at very high ion concentrations due to intrinsic structural properties of the channel or presence of blockers. Instead, conductance curves obey simple saturation kinetics that follow a Michaelis–Menten relationship (Hille 2001) (Figure 1.6). The typical conductance–concentration saturation curve is comprised of two components: an initial quasi-linear rise at low ion concentrations and a plateau at higher ion concentrations (Latorre and Miller 1983) (Figure 1.6A). The initial linear slope of the curve measures the rate of ion entry into the pore. The plateau portion of the curve represents the maximum conductance—or g_{max}—and is a measure of the exit rate of the permeating ion. Saturation occurs when the steps of ion binding and unbinding are rate limiting. At high ion concentrations, the rate of ion entry increases and it will approach the maximum rates of unbinding (Hille 2001). Therefore, as ion concentrations increase further, the rates of unbinding determine the overall rate of conduction and a plateau at maximum conductance is reached. Intrinsic properties of the ion channel alter this maximum conductance by changing the rate-limiting step of ion exit from the pore.

The absolute upper limit of conductance is set by the diffusion of ions into the mouth of the pore and can be quantified by the phenomena of convergence conductance (Latorre and Miller 1983). The convergence conductance depends on the proportion of the size of the pore to the radius of the permeant ion. The intimate contact between the ion and the

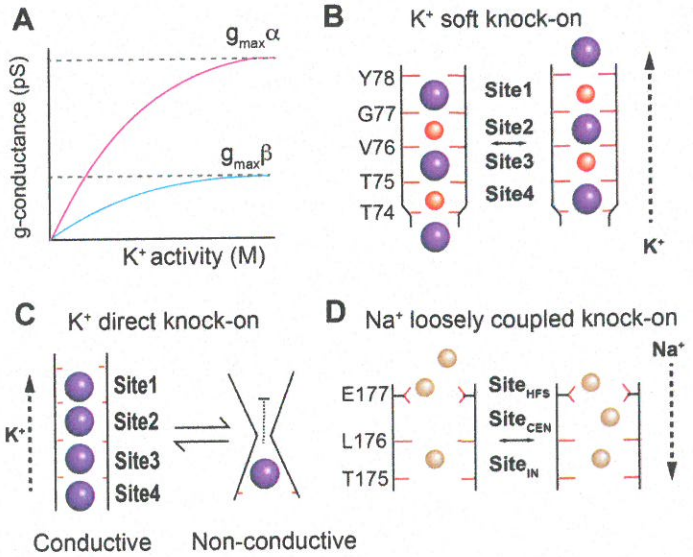

FIGURE 1.6
Ion channel conduction mechanisms. (A) Theoretical graph showing conductance as a function of ionic activity for hypothetical channel α with high maximum conductance (g_{max}) such as KcsA (magenta curve) and for hypothetical channel β with low g_{max} such as K_{ir} (blue curve). The g_{max} for each channel is denoted by a dotted black line. (B) The soft knock-on model for K^+ channel. (C) Transition between conductive selectivity filter (four fully occupied ion-binding sites) and nonconductive (or collapsed) selectivity filter (with one ion-binding site). (D) The loosely coupled knock-on model for Na^+ channel, based on the molecular dynamics simulation analysis of prokaryotic Na_vAb channels. (The illustrations are adapted based on DeMarco, Bekker, and Vorobyov 2019.)

pore walls essential for high selectivity would be antithetical to a large convergence conductance ratio representative of a wide pore radius to small ionic radius (Bezanilla and Armstrong 1972). Paradoxically, K^+ channels can have very high conduction rates while also being highly selective. To circumvent this issue, the specific energetic landscapes embedded by various molecular properties along the permeation pathway have been tailored. Channels will primarily maintain a narrow constriction at the selectivity filter to ensure high ion selectivity—in some instances forcing ion–ion interactions influencing conductance characteristics—but also widen the pore at the base in order to increase the entry rate and promote higher conductance.

A series of mechanisms hypothesized to accommodate the balance of high selectivity and large conductance is centered on the multi-ion theory, postulating the pore's capacity to occupy multiple ions at the same time in a single file. In the multi-ion pore, repulsion between ions increases the exit rate of ions from the pore, enhancing g_{max} (Hille 2001). A model for the barrier-less conduction in K^+ channels was proposed based on the observed configurations of the selectivity filter obtained in different ionic concentrations with X-ray crystallography (Morais-Cabral, Zhou, and MacKinnon 2001; Zhou et al. 2001). In high permeant ion concentrations, the selectivity filter was found in a conductive state, where two ions can bind at the same time in either a water–K–water–K (S2, S4) or K–water–K–water (S1, S3) configuration that follows a soft, or water-mediated, knock-on model (Figure 1.6B). Permeating ions provide counter charges for the 20 electronegative oxygen atoms to stabilize the filter while minimizing the destabilization from same charge repulsion. Under the knock-on model, entry of an additional ion would destabilize this configuration providing the necessary energy to transport the ion creating a mechanism for coupling high conductivity with high selectivity. Molecular dynamics simulations more recently challenged this model with evidence of a water-free selectivity filter that may be fully occupied in a K–K–K–K configuration in support of a direct knock-on model (Kopfer et al. 2014) (Figure 1.6C). At low permeant ion concentrations, the KcsA selectivity filter assumes a collapsed and nonconductive conformation with presumably only one ion bound at one time (Morais-Cabral, Zhou, and MacKinnon 2001). In the collapsed KcsA, a conformational change leads to a lower ion-binding affinity and increases the exit rate of bound ions. Because the nonconductive filter contains only one ion, the second ion-binding event is presumed to rebound the filter from a collapsed to a conductive conformation (Figure 1.6C). This study illustrates yet another possibility of how high selectivity could coexist with high conduction. The presence of multiple high affinity binding sites in the pore allows for selection of certain ions over others, while high conduction only occurs in the occupied selectivity filter due to both electrostatic repulsion. Interestingly, the relationship between ion-binding affinity and selectivity filter conformation as a factor in channel conductance is further supported by studies with MthK, a K^+ channel from the archaea *Methanobacterium thermoautotrophicum*. MthK—which will be discussed as a member of a K^+ channel class that exhibits the largest known conductances—is unlike KcsA because it does not show a collapsed selectivity filter in low concentrations of permeant ions (Ye, Li, and Jiang 2010). Moreover, the MthK selectivity filter was shown to possess higher K^+ binding affinity and consequently a higher probability of binding multiple ions and adopt a conductive state versus a nonconductive one (Boiteux et al. 2020).

The selectivity filter in the Na_v channel likewise follows a multi-ion pore occupancy, but a significantly wider pore than the K^+ channel leads to different permeation mechanisms (DeMarco, Bekker, and Vorobyov 2019). Molecular dynamics simulations of ion permeation in the bacterial voltage-gated Na^+ channel Na_vAb, which harbors a conserved selectivity filter motif to Na_vMs (shown in Figure 1.4E, F), propose a "loosely coupled knock-on"

mechanism (Figure 1.6D). In this model, three ion-binding sites impose individual energy barriers and orchestrate to discriminate between ions. Na^+ can move freely between a high-field-strength binding site ($Site_{HFS}$) located toward the extracellular side—designated by a negatively charged glutamate side chain as well as the nearby serine—and a binding site located more toward the internal cavity ($Site_{IN}$)—where it is fully hydrated and coordinated by the backbone carbonyl oxygens pointing into the pore. However, a central binding site ($Site_{CEN}$) located between the external and internal sites is proposed to be the largest energy barrier impeding the permeation of two ions already bound in the selectivity filter. Simulations suggest trapped ions at $Site_{HFS}$ and $Site_{IN}$ can permeate upon an additional ion entering from the extracellular side (Boiteux, Vorobyov, and Allen 2014).

In contrast, attractive forces at ion-binding sites available to multiple ion occupants have been shown to decrease the rate of exit—thus decreasing conductance—as exemplified by the anomalous mole fraction effect. The anomalous mole fraction effect describes changes in permeability ratios of Na^+, K^+ and Ca^{2+} through a common pore when more than one permeant ion type is present (Hess and Tsien 1984; Almers and McCleskey 1984). In certain channels, the conductance passes through a minimum or maximum when plotted against the mole fraction of two permeant ions, and it was understood to occur by allowing the two ions to interact inside the pore and with the pore walls (Nonner, Chen, and Eisenberg 1998) (Figure 1.7). When Hodgkin and Keynes first observed anomalous unidirectional flux ratios in squid axons and offered an explanation by flux coupling, it marked a critical deviation from the expectation that ions pass through independently of one another thereby opening ideas on ion–ion interaction to take hold (Hodgkin and Keynes 1955).

While ion selectivity varies little within a channel subfamily, conductance levels can vary dramatically. Some K^+ channels exhibit a low conductance approximating 10 pS, including inward-rectifying K^+ channels (K_{ir}), K_v, and small-conductance K^+ (SK) channels (Latorre and Miller 1983). In similar conditions, "maxi-K" channels such as the Ca^{2+}-dependent large-conductance K^+ (BK) channels and their archaeal homolog MthK exhibit the largest conductance levels of 100-400 pS that is nearing the diffusion limit ranging from 250 to 300 pS (Zadek and Nimigean 2006; Eisenman, Latorre, and Miller 1986; Latorre and Miller 1983). Since the selectivity filter of different K^+ channels is highly conserved, other factors must account for these varying levels of conductance that can be roughly 10–20 times

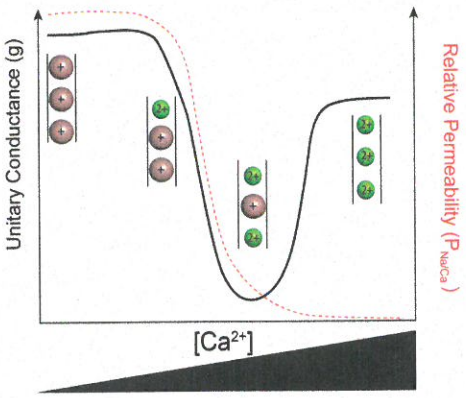

FIGURE 1.7
Anomalous mole fraction. Anomalous mole fraction effect of a cation channel permeable to Na^+ and Ca^{2+} illustrating changes to a channel's unitary conductance (solid black line) and relative permeability (dashed red line) as two competing ions enter the pore. Na^+ concentration remains constant against increasing Ca^{2+} concentrations. Na^+ ions are presented as tan spheres and Ca^{2+} ions as green spheres.

higher in BK/MthK than other K^+ channels (Figure 1.8). One determinant of conductance in K^+ channels is the size of the inner cavity entrance where K^+ ions need to pass through before entering the selectivity filter from the intracellular side. Structures of MthK and BK channels revealed that these channels contain a large aqueous cavity at the inner mouth of the pore measuring 16–20 Å directly under the selectivity filter (Fan et al. 2020; Hite, Tao, and MacKinnon 2017). This cavity is larger than the equivalent in other K^+ channels, such as KcsA and K_v channels, which contain a more modestly sized vestibule (8–12 Å) and correspondingly smaller conductances (10–60 pS) (Doyle et al. 1998; Long, Campbell, and Mackinnon 2005; LeMasurier, Heginbotham, and Miller 2001) (Figure 1.8A–D). The importance of the inner cavity entrance size was supported by studies showing that an increase of side chain volume at the cavity entrance results in a reduction of single-channel conductance in the outward direction, while having no effect on the inward current (Brelidze

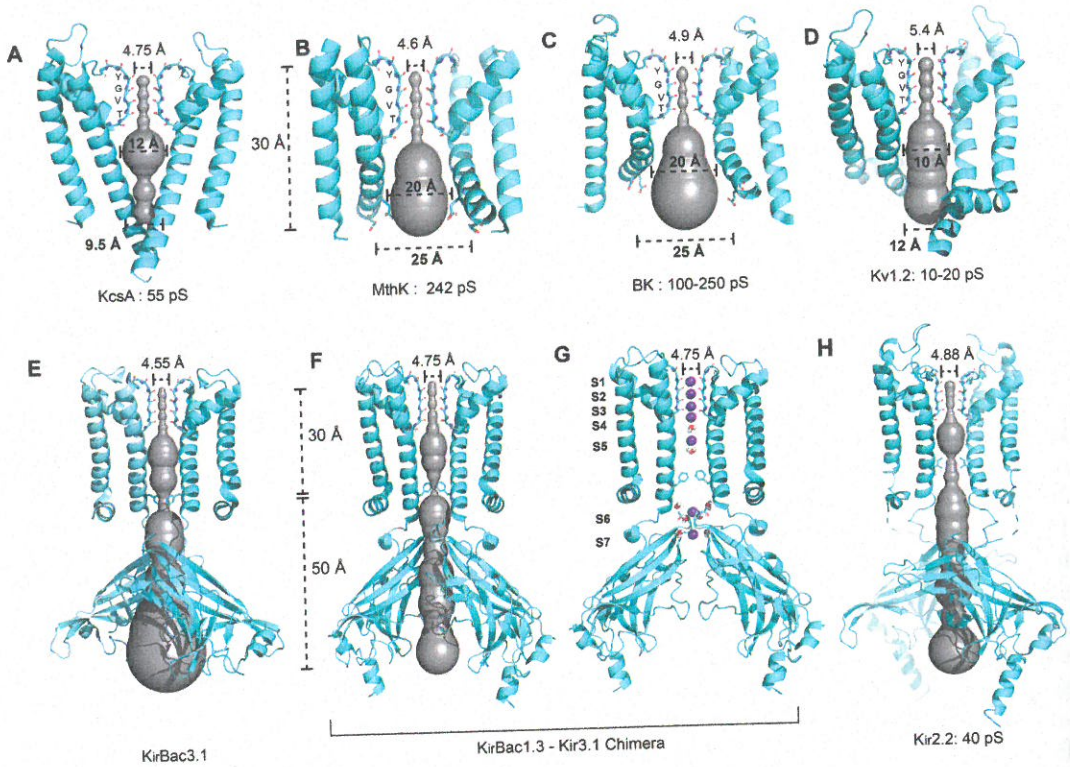

FIGURE 1.8
Pore cavity dimensions and conductance. (A–D) Representation of the pore cavity in K^+ channels: (A) KcsA (PDB: 1K4C), (B) MthK (PDB: 4HYO), (C) the BK channel encoded by the gene *Slo1* (PDB: 6V38) and (D) $K_v1.2$ (PDB: 2A79). Dashed bars on ion channel structures denote the average width between opposing subunits in the selectivity filter (between carbonyl oxygens), the width of the intermediate cavity, and the width of the cytosolic entrance. Please note that cavity dimensions between opposing subunits extend into the z-axis. (E, F and H) Representation of the pore cavity for (E) K_{ir}Bac3.1 (PDB: 4LP8), (F) a chimera composed of the K_{ir}Bac1.3 transmembrane portion joined to K_{ir}3.1 residues that interface the membrane plus cytosolic domains (PDB: 2QKS), and (H) K_{ir}2.2 (PDB: 3JYC). Note the upper portion of the pore comprising the selectivity filter remains similarly narrow to other K^+ channels of all conductance levels while inner cavities vary in dimensions. (G) Molecular representation of K_{ir}Bac1.3–K_{ir}3.1 showing two opposing subunits illustrating that the formation of a long pore includes the possible formation of two additional K^+ ion-binding sites, not present in KcsA (shown in Figure 1.2). Similar to the chimeric channel, K_{ir}Bac3.1 and K_{ir}2.2 also show additional K^+ ions in the C-terminal portion. Front and back subunits have been removed for clarity in all panels.

and Magleby 2005). The reduction in outward current could be reversed by an increase in intracellular K^+ concentration (Geng, Niu, and Magleby 2011). This suggests that the ions do not encounter a barrier upon entrance into the cavity of these channels, which contributes to the increase in conduction rate. Molecular dynamics simulations provide further support for the importance of the cavity width to conductance as K^+ channel conductance increased with a widening of the entrance to the inner vestibule (Chung, Allen, and Kuyucak 2002). In addition, eight negative charges ring the entrance of BK/MthK to attract K^+ ions to the cavity, which was proposed to elevate the local K^+ concentration, and enhances channel conductance as predicted by the conductance–concentration curve (Nimigean, Chappie, and Miller 2003) (Figure 1.8B).

In addition to cavity size, pore length has been hypothesized to contribute to the single-channel conductance level (Latorre and Miller 1983). This hypothesis is consistent with structural and functional studies of the bacterial inward-rectifying K^+ channels (K_{ir}Bac) and the eukaryotic $K_{ir}2.2$. K_{ir} channels exhibit a relatively low conductance level of ~10–35 pS at –100 mV for KirBac1.1 and to 40 pS at –80 mV for $K_{ir}2.2$ (Cheng, Enkvetchakul, and Nichols 2009; Tao et al. 2009). K_{ir} channels are structurally characterized in part by a pore that is ~50–85 Å in length that extends through its large C-terminal domain (Bavro et al. 2012; Tao et al. 2009; Nishida et al. 2007) (Figure 1.8E–H). By comparison, many prokaryotic (KcsA, Mthk) and eukaryotic (Shaker/K_v, BK) channels have a typical pore length of 30 Å (Doyle et al. 1998; Long, Campbell, and Mackinnon 2005; Posson, McCoy, and Nimigean 2013) (Figure 1.8A–D). Nonetheless, channel families such as the Shaker/K_v channels and SK channels also display a low single-channel conductance level (10–20 pS) without a similarly long pore to K_{ir} suggesting the elongated pore harbors additional electrochemical features that strengthen barriers in the energetic landscape. Whether the molecular properties dampening conductance rates are conserved across K^+ channel families remains to be determined. Modifications at the molecular level in pore chemistry, electrostatics, and pore dimensions peripheral to the evolutionarily conserved selectivity filter enables an array of conductance levels. Ultimately, the interplay among a network of ion channels along the same membrane with different ion selectivity and conductance rates cooperate to command the membrane potential for electrical signaling.

Suggested Readings

This chapter includes additional bibliographical references hosted only online as indicated by citations in blue color font in the text. Please visit https://www.routledge.com/9780367538163 to access the additional references for this chapter, found under "Support Material" at the bottom of the page.

Almers, W., and E. W. McCleskey. 1984. "Non-selective conductance in calcium channels of frog muscle: calcium selectivity in a single-file pore." *J Physiol* 353:585–608. doi:10.1113/jphysiol.1984.sp015352.

Bezanilla, F., and C. M. Armstrong. 1972. "Negative conductance caused by entry of sodium and cesium ions into the potassium channels of squid axons." *J Gen Physiol* 60 (5):588–608.

Boiteux, C., D. J. Posson, T. W. Allen, and C. M. Nimigean. 2020. "Selectivity filter ion binding affinity determines inactivation in a potassium channel." *Proc Natl Acad Sci U S A* 117 (47):29968–78. doi:10.1073/pnas.2009624117.

Cheng, W. W., J. G. McCoy, A. N. Thompson, C. G. Nichols, and C. M. Nimigean. 2011. "Mechanism for selectivity-inactivation coupling in KcsA potassium channels." *Proc Natl Acad Sci U S A* 108 (13):5272–7. doi:10.1073/pnas.1014186108.

Derebe, M. G., D. B. Sauer, W. Zeng, A. Alam, N. Shi, and Y. Jiang. 2011. "Tuning the ion selectivity of tetrameric cation channels by changing the number of ion binding sites." *Proc Natl Acad Sci U S A* 108 (2):598–602. doi:10.1073/pnas.1013636108.

Doyle, D. A., J. Morais Cabral, R. A. Pfuetzner, A. Kuo, J. M. Gulbis, S. L. Cohen, B. T. Chait, and R. MacKinnon. 1998. "The structure of the potassium channel: molecular basis of K+ conduction and selectivity." *Science* 280 (5360):69–77. doi:10.1126/science.280.5360.69.

Dwyer, T. M., D. J. Adams, and B. Hille. 1980. "The permeability of the endplate channel to organic cations in frog muscle." *J Gen Physiol* 75 (5):469–92. doi:10.1085/jgp.75.5.469.

Eisenman, G. 1962. "Cation selective glass electrodes and their mode of operation." *Biophys J* 2 (2 Pt 2):259–323. doi:10.1016/s0006-3495(62)86959-8.

Eisenman, G., R. Latorre, and C. Miller. 1986. "Multi-ion conduction and selectivity in the high-conductance Ca++-activated K+ channel from skeletal muscle." *Biophys J* 50 (6):1025–34. doi:10.1016/S0006-3495(86)83546-9.

Fan, C., N. Sukomon, E. Flood, J. Rheinberger, T. W. Allen, and C. M. Nimigean. 2020. "Ball-and-chain inactivation in a calcium-gated potassium channel." *Nature* 580 (7802):288–93. doi:10.1038/s41586-020-2116-0.

Geng, Y., X. Niu, and K. L. Magleby. 2011. "Low resistance, large dimension entrance to the inner cavity of BK channels determined by changing side-chain volume." *J Gen Physiol* 137 (6):533–48. doi:10.1085/jgp.201110616.

Heginbotham, L., Z. Lu, T. Abramson, and R. MacKinnon. 1994. "Mutations in the K+ channel signature sequence." *Biophys J* 66 (4):1061–7. doi:10.1016/S0006-3495(94)80887-2.

Hille, B. 2001. *Ion channels of excitable membranes*. 3rd ed. Sunderland, MA: Sinauer Associates, Inc.

Hite, R. K., X. Tao, and R. MacKinnon. 2017. "Structural basis for gating the high-conductance Ca(2+)-activated K(+) channel." *Nature* 541 (7635):52–7. doi:10.1038/nature20775.

Hodgkin, A. L., and A. F. Huxley. 1952. "Currents carried by sodium and potassium ions through the membrane of the giant axon of Loligo." *J Physiol* 116 (4):449–72. doi:10.1113/jphysiol.1952.sp004717.

Hodgkin, A. L., and R. D. Keynes. 1955. "The potassium permeability of a giant nerve fibre." *J Physiol* 128 (1):61–88.

Kopfer, D. A., C. Song, T. Gruene, G. M. Sheldrick, U. Zachariae, and B. L. de Groot. 2014. "Ion permeation in K(+) channels occurs by direct Coulomb knock-on." *Science* 346 (6207):352–5. doi:10.1126/science.1254840.

Latorre, R., and C. Miller. 1983. "Conduction and selectivity in potassium channels." *J Membr Biol* 71 (1–2):11–30.

Long, S. B., E. B. Campbell, and R. Mackinnon. 2005. "Voltage sensor of Kv1.2: structural basis of electromechanical coupling." *Science* 309 (5736):903–8. doi:10.1126/science.1116270.

Neher, E., and B. Sakmann. 1976. "Single-channel currents recorded from membrane of denervated frog muscle fibres." *Nature* 260 (5554):799–802. doi:10.1038/260799a0.

Noda, M., S. Shimizu, T. Tanabe, T. Takai, T. Kayano, T. Ikeda, H. Takahashi, H. Nakayama, Y. Kanaoka, N. Minamino, et al. 1984. "Primary structure of Electrophorus electricus sodium channel deduced from cDNA sequence." *Nature* 312 (5990):121–7. doi:10.1038/312121a0.

Noskov, S. Y., S. Berneche, and B. Roux. 2004. "Control of ion selectivity in potassium channels by electrostatic and dynamic properties of carbonyl ligands." *Nature* 431 (7010):830–4. doi:10.1038/nature02943.

Pan, X., Z. Li, Q. Zhou, H. Shen, K. Wu, X. Huang, J. Chen, J. Zhang, X. Zhu, J. Lei, W. Xiong, H. Gong, B. Xiao, and N. Yan. 2018. "Structure of the human voltage-gated sodium channel Nav1.4 in complex with beta1." *Science* 362 (6412). doi:10.1126/science.aau2486.

Papazian, D. M., T. L. Schwarz, B. L. Tempel, Y. N. Jan, and L. Y. Jan. 1987. "Cloning of genomic and complementary DNA from Shaker, a putative potassium channel gene from Drosophila." *Science* 237 (4816):749–53. doi:10.1126/science.2441470.

Payandeh, J., T. Scheuer, N. Zheng, and W. A. Catterall. 2011. "The crystal structure of a voltage-gated sodium channel." *Nature* 475 (7356):353–8. doi:10.1038/nature10238.

Shi, N., S. Ye, A. Alam, L. Chen, and Y. Jiang. 2006. "Atomic structure of a Na+- and K+-conducting channel." *Nature* 440 (7083):570–4. doi:10.1038/nature04508.

Starkus, J. G., L. Kuschel, M. D. Rayner, and S. H. Heinemann. 1997. "Ion conduction through C-type inactivated Shaker channels." *J Gen Physiol* 110 (5):539–50. doi:10.1085/jgp.110.5.539.

Thompson, A. N., I. Kim, T. D. Panosian, T. M. Iverson, T. W. Allen, and C. M. Nimigean. 2009. "Mechanism of potassium-channel selectivity revealed by Na(+) and Li(+) binding sites within the KcsA pore." *Nat Struct Mol Biol* 16 (12):1317–24. doi:10.1038/nsmb.1703.

Varma, S., D. Sabo, and S. B. Rempe. 2008. "K+/Na+ selectivity in K channels and valinomycin: over-coordination versus cavity-size constraints." *J Mol Biol* 376 (1):13–22. doi:10.1016/j.jmb.2007.11.059.

Zhou, Y., J. H. Morais-Cabral, A. Kaufman, and R. MacKinnon. 2001. "Chemistry of ion coordination and hydration revealed by a K+ channel-Fab complex at 2.0 A resolution." *Nature* 414 (6859):43–8. doi:10.1038/35102009.